Open Archive TOULOUSE Archive Ouverte (OATAO)

Identification of ageing biomarkers in human dermis biopsies by thermal analysis (DSC) combined with Fourier transform infrared spectroscopy (FTIR/ATR)

R. Tang[1] | V. Samouillan[1] | J. Dandurand[1] | C. Lacabanne[1] |
M-H. Lacoste-Ferre[1] | P. Bogdanowicz[2] | P. Bianchi[2] | A. Villaret[2] | F. Nadal-Wollbold[2]

[1]CIRIMAT, Paul Sabatier University, Toulouse, France

[2]Pierre Fabre Dermo Cosmetique, Toulouse, France

Correspondence
Valarie Samouillan, CIRIMAT, Paul Sabatier University, Toulouse, France.
Email: valerie.samouillan@univ-tlse3.fr

Background/purpose: The purpose of this clinical study was to identify suitable biomarkers for a better understanding of the molecular and organizational changes in human dermis during intrinsic and extrinsic ageing.

Methods: Sun-exposed and non-exposed skin biopsies were collected from twenty-eight women devised in two groups (20-30 and ≥60 years old). The hydric organization and thermal transitions were determined by Differential Scanning Calorimetry (DSC). Fourier Transform Infrared spectroscopy (FTIR) was used to identify the absorption bands of the dermis and to quantify the different absorbance ratio.

Results: The amounts of total, freezable and unfreezable water were determined. A significant increasing amount of freezable water is evidenced in sun-exposed area skin of aged group compared with young group (P=.0126). Another significant effect of extrinsic ageing (P=.0489) is the drastic decrease of fibrillary collagen, the main protein component of dermis. The only significant effect of intrinsic ageing (P=.0184) is an increase of the heat-stable fraction of collagens in dermis.

Conclusion: DSC and FTIR are well-suited techniques to characterize human skin, giving accurate results with a high reproducibility. The combination of these techniques is useful for a better understanding of human skin modifications with intrinsic and extrinsic ageing.

KEYWORDS
collagen denaturation, differential scanning calorimetry, Fourier transform infrared spectroscopy, human skin ageing, hydration, secondary structures of proteins

1 | INTRODUCTION

Skin ageing is a combination of chronological processes and external factors (as sun exposition). Wrinkles are the major macroscopic sign of skin ageing resulting from molecular modification of dermis.

Among the various components of the dermis, extracellular matrix consisting of collagens, elastic fibres and amorphous ground substances is strongly involved in the process of cutaneous ageing,[1] in close correlation with changes in hydration.[2,3] Collagen, the most abundant component in the dermis, comprises 80% of the tissue total dry mass and 90% of all dermal proteins. Collagens I and III represent close to 90% and 10%, respectively, in the composition of dermal collagen fibrils. Altogether, the fibrils with their associated proteins confer tensile strength to the skin and are pivotal for the general organization and stability of the dermal extracellular matrix among other functions.[4]

A great number of clinical studies have been performed on skin biopsies to help the understanding on mechanisms involved

in chronological (intrinsic) and photo (extrinsic) ageing [5,6] using histological and ultrastructural approaches. Unfortunately, the complexity and slowness of the ageing processes leading to subtle changes of biological function provide the ageing research with enormous difficulties.

Although new information on whole skin and dermis can be reached at the molecular level through near-infrared diffusive-reflection (NIR-DR),[7] attenuated total reflectance Fourier transform infrared spectroscopy (ATR-FTIR),[7,8] Raman spectroscopy,[9,10] nuclear magnetic resonance/magnetic resonance imaging (NMR/MRI),[8,11] dynamic vapour sorption (DVS),[12] changes in dermis hydration with age yield somewhat conflicting results, which could be attributed to the preparation of samples.

Combined with thermogravimetric analysis (TG) measurements, differential scanning calorimetry (DSC) is a standard method to evaluate freezable and unfreezable water.[13] DSC is also an appropriate method for assessing protein thermal stability and conformational changes. It is particularly well-suited to evaluate the thermal stability of purified collagens in solution or in their aggregated form,[14] or directly in native tissues.[15,16] It has been successfully applied to characterize collagen both in animal and human skins.[16-19] In our previous work [20] on skin explants, we validated the combined use of DSC and FTIR techniques to obtain suitable biomarkers of the hydric organization and biomacromolecules integrity.

The aim of this work was to evaluate, for the first time, chronological and photo-ageing with these techniques in a clinical study on biopsies from two age groups (20-30 and >60 years old).

2 | MATERIALS AND METHODS

2.1 | Study design and patients selection

This monocentric, comparative, open, study was conducted at the Pierre Fabre Skin Research Centre—CRP, Toulouse (France), in accordance with the ethical principles of the Declaration of Helsinki and Good Clinical Practice guidelines. The protocol was approved by the Sud-Ouest et Outre Mer III Committee for the Protection of Persons (Ethics Committee, N° ID RCB 2014-A00698-39) and the French Health Products Safety Agency (ANSM). Each volunteer signed a written informed consent.

Twenty eight healthy female volunteers divided in two groups: aged 20–30 years and ≥60 years old with a SCINEXA score, respectively, < and ≥ at 2. SCINEXA (SCore for INtrinsic and EXtrinsic skin Ageing) is a parameter which evaluate and differentiate intrinsic (<2) and extrinsic (≥2) ageing.

2.2 | Samples treatment

Two four mm punch biopsies were taken from each volunteer: on sun-protected left buttock and left dorsal forearm resulting in four series: Young sun-Protected (YP), Aged sun-Protected (AP), Young sun-Exposed (YE) and Aged sun-Exposed (AE). The skin biopsy procedure was performed by a suitably qualified medical specialist. Samples were immediately rinsed in Phosphate Buffered Saline solution, frozen in liquid nitrogen and stored at −20°C. We performed stepwise thawing of the explants, (1st stage at 5°C for 24 hours, and 2nd stage at 20°C for 10 minutes) until DSC and FTIR analysis.

2.3 | Differential Scanning Calorimetry

Differential scanning calorimetry (DSC) measurements were performed with a DSC Pyris calorimeter (Perkin Elmer, Waltham, MA, USA) using an empty pan as reference. The calorimeter was calibrated using the manufacturer's instructions with pure water, cyclohexane and Indium as standards, resulting in a temperature accuracy of ±0.1°C and an enthalpy accuracy of ±0.2 J g^{-1}. Temperature calibration was undertaken at each scanning rate. Skin biopsies (5-8 mg by mass) were sealed in hermetic aluminium pan. Samples were cooled at 10°C min^{-1} to −30°C (1st cooling scan), then held 10 minutes to freeze water.

To determine freezable water amount and intrinsic thermal transitions, the samples were heated at 10°C min^{-1} to 85°C (1st heating scan), then cooled at −10°C min^{-1} to −30°C and then heated at 10°C min^{-1} to 85°C (2nd heating scan).

After completing the DSC measurements, pans were reweighted to check that they had been correctly sealed. The sample pans were pierced and dried to constant mass at 195°C for 10 minutes to determine the sample dry mass and the total water mass.

2.4 | Fourier Transform Infrared analysis (FTIR)

FTIR/ATR spectra were acquired using a Nicolet 5700 FTIR (Thermo Fisher Scientific, Waltham, MA, USA) equipped in ATR device with a KBr beam splitter and a MCT/B detector. Explants (dermis face) were directly laid on the ATR accessory (Smart Orbit with a type IIA diamond crystal) and covered by a hermetic cap with an "O" ring to avoid dehydration of the sample during spectra acquisition. Spectra were recorded over the region of 4000–450 cm^{-1} with a spectral resolution of 1 cm^{-1} and 80 accumulations. Spectral data were collected using Omnic 8.0 (Thermo Fisher Scientific). After background subtraction and baseline correction achieved on Omnic 8.0 (Thermo Fisher Scientific), spectral data were normalized in the amide II region. For each series, a mean representative spectrum was computed. Second derivatives and Fourier-Self-Deconvolution (FSD) were used to enhance the chemical information present in overlapping infrared absorption bands.

2.5 | Statistical analysis

Quantitative values are shown as mean±SEM. Statistical analysis have been done with SA software. Wilcoxon-Mann-Whitney test has been used to compare data between groups and Wilcoxon signed-rank test to compare data between areas (sun-protected and sun-exposed) from the same group. It was considered statistically significant threshold of P-value less than .05.

3 | RESULTS AND DISCUSSION

3.1 | Thermal characterization

In Figure 1 are reported the DSC curves (normalized to the initial mass) of a skin biopsy in the sun-protected zone of a young subject.

3.2 | Water quantification

The endothermic peaks recorded in the [−20; 20°C] zone correspond to the melting of freezable water. This extrinsic transition is widely used to quantify the amount of total freezable water in hydrated proteins and tissues (by dividing the area of the measured endothermic peak by 334 J g^{-1}, corresponding to the melting enthalpy of pure ice at 0°C),[21] and completes thermogravimetric analyses giving the total amount of water. The amount of unfreezable water can be calculated by a simple difference. These quantifications were performed for all the samples and reported in Table 1.

The total hydration of human skin biopsies is consistent with literature data,[22] giving an average value of 70% for the hydration of human dermis and epidermis. This remarkably high value is due to a combination of physical and chemical factors including the presence of interconnected gaps, the particularly hygroscopic nature of hyaluronic acid and the hydrophilicity of collagen. If a well-documented literature is available for the total hydration of stratum corneum, epidermis and dermis,[3] few data, obtained from Raman spectroscopy,[10] DVS,[12] NMR [11] are reported on the indirect quantification of the different kinds of water (namely free and bound water) in human skin. In a preliminary study on human abdominal skin biopsies [20] we justified the use of the terms freezable/unfreezable water instead of free/bound water rather reserved to vibrational or relaxational techniques. The present DSC study shows that the freezable water (that covers bulk water in excess but also confined water in mesopores) roughly represents two-third of the total water in human skin in accordance with previous NMR, DVS, and DSC results.[11,12,20,23] One-third of the total water of human skin is unfreezable water, corresponding to the filling of the first hydration shell of proteins and other hydrophilic components.

There is a significant increasing amount of freezable water in AE series compared with YE group (56.2% vs 48.4%, P=.0126), associated with a decrease amount of unfreezable water (21.0% vs 23.7%, P=.0599), causing a very significant decrease (0.374 vs 0.490, P=.0039) of the ratio of unfreezable water to freezable water.

Between two areas of the aged groups, we note a similar tendency for the different water structures, highlighting the preponderant effect of extrinsic ageing on the hydric organization of the skin.

No significant differences are found between the amounts of total, freezable and unfreezable water of YP and AP skins, what also implies a similar ratio of unfreezable water to freezable water. We can assume that chronological intrinsic ageing only does not give rise to the alteration of the hydric structures.

It can be noticed that no significant difference are found between the hydric organization of YP and YE groups. The comparison is less straightforward in this case, since it deals with two anatomically different zones—buttocks and forearms—that may bias the final data.

Our results can be connected with previous Raman studies [10] evidencing (1) water structures and amount were similar in sun-exposed and sun-protected regions of young skin and (2) water structures and amount were similar in the chronologically aged skin compared with young skin. Last but not least, our results showed an increased content of total and non-bounded water in the photoaged skin.

Gniadecka et al. highlighted a decrease on echogenicity in the upper dermis of sun-exposed region in photoaged skin, that could be
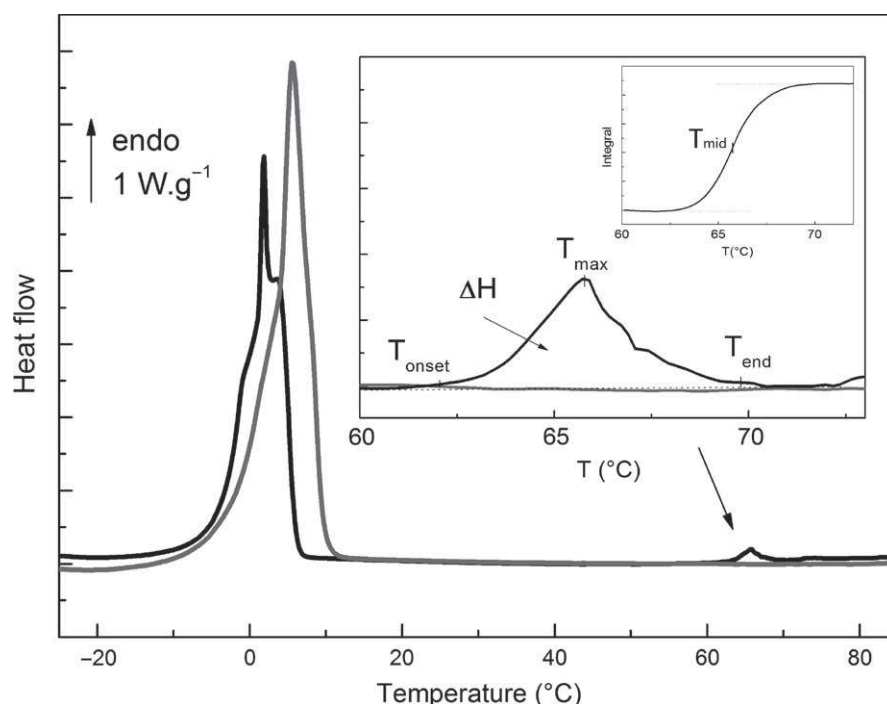

FIGURE 1 DSC curves of a skin biopsy from the 20-30 years old group, sun-protected zone (first and second heating, scanning rate 10°C min^{-1}, and enlargement in the [60-85°C] window)

TABLE 1 Amounts of total, freezable and unfreezable water in four skin series: Young sun-Protected (YP), Aged sun-Protected (AP), Young sun-Exposed (YE) and Aged sun-Exposed (AE). Significant difference was noted as follows: [a]YE vs AE (P=.0126), [b]AP vs AE (P=.0156), [c]AP vs AE (P=.0469), [d]YE vs AE (P=.0039) and [e]AP vs AE (P=.0116)

Skin samples	% Total water	% Freezable water	% Unfreezable water	Ratio unfreezable/freezable water
YP	75.2±1.7	51.4±1.3	23.8±1.6	0.466±0.038
YE	72.1±1.5	48.4±1.2[a]	23.7±0.7	0.490±0.017[d]
AP	76.3±1.1	52.7±0.9[b]	23.6±0.6[c]	0.448±0.013[e]
AE	77.2±0.6	56.2±0.7[a,b]	21.0±0.7[c]	0.374±0.016[d,e]

due to a degradation of collagen, accumulation of GAGs and water in the upper dermis leading to an increased content of total and non-bounded water.[10,24]

It must be reminded that the collagen secondary structure is stabilized by both intra- and inter-chain water bridges with carbonyl and hydroxyprolyl groups.[25] Thus, despite an increase of the total water content, the decrease in the bounded-water content (protein-water interactions) will lead to the instability and fragmentation of collagen fibrils.[26]

3.3 | Collagen denaturation

Enlargement of Figure 1 shows the DSC curves of a sun-protected skin biopsy of a young subject in the 60-85°C zone. The endothermic phenomenon recorded in this temperature zone during the first heating is associated with the irreversible thermal denaturation of type I and type III collagens.[20] The collagen denaturation—distinct from degradation—is a thermally activated process that involves rupture of hydrogen bonds coupling the three α-chains and a rearrangement of the triple helix into a random chain configuration.[14]

As shown on Figure 1, the main characteristics of the denaturation peak are T_{onset}, T_{max}, T_{mid}, T_{end} and the area under the endotherm peak. T_{mid} represents the temperature at which 50% of collagen is denatured and it is computed from the integral of the denaturation endotherm.

T_{onset} and T_{end} are computed from a fixed threshold value of the signal first derivative. T_{onset}, T_{max}, T_{mid} are alternatively taken as the denaturation temperature according to the previous studies [15,17,19] while T_{end}, also known as the "recovery temperature" can be used to take into account the widening of the collagen thermal denaturation under certain conditions.[17] ΔH, once normalized to the dry mass, gives a measure of the specific heat/enthalpy of denaturation. We reported in Figure 2 the mean values of T_{mid} (2A) and T_{end} (2B) for the different series of biopsies. The T_{mid} temperature is located at 67°C for the sun-protected biopsies of young subjects (YP). It fits with the temperature denaturation range of skins from animals [16] or abdominal human skins.[20] It is known that the denaturation temperature drastically increases as the hydration decreases,[15] due to the decrease of intrafibrillar water and to the replacement of protein-protein hydrogen bonds by protein-water hydrogen bonds. This temperature becomes independent upon hydration above 1 kg of water per kg of dry tissue,[16] what is checked for the studied samples, with a total amount of water of 3 kg per kg of dry mass. In this case, the denaturation temperature can be considered as an intrinsic characteristic of collagens in the skin and can be compared to each other regardless of hydration.

Even if the mean value of T_{mid} is slightly depressed in the sun-exposed aged skin (AE, T_{mid}=66.5°C) no significant difference (P=.0836) is found with the sun-exposed young skin (YE, T_{mid}=68.0°C). Nevertheless, the decrease of T_{mid} is significant between the
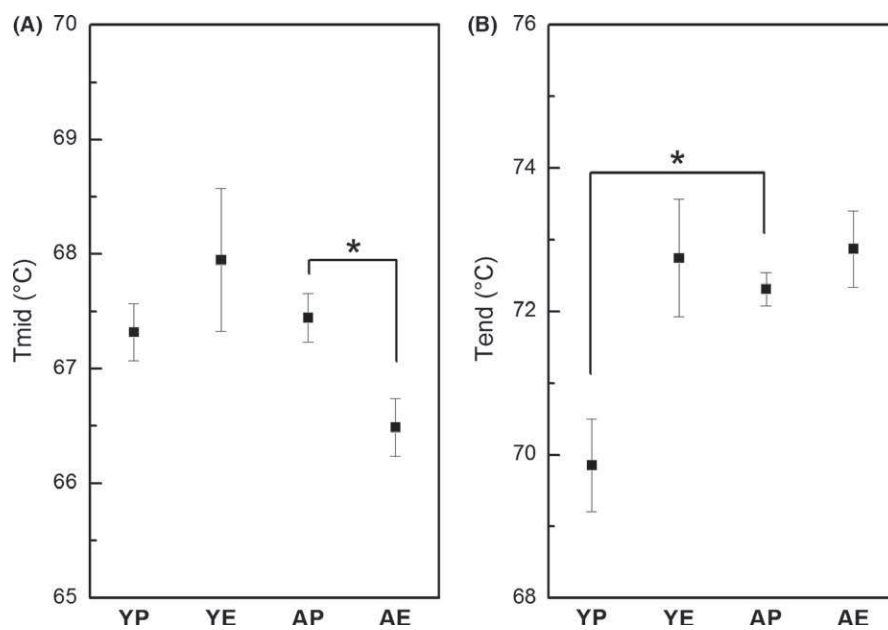

FIGURE 2 Main thermal characteristics of the denaturation endotherm in skin biopsies: A, T_{mid} and B, T_{end}
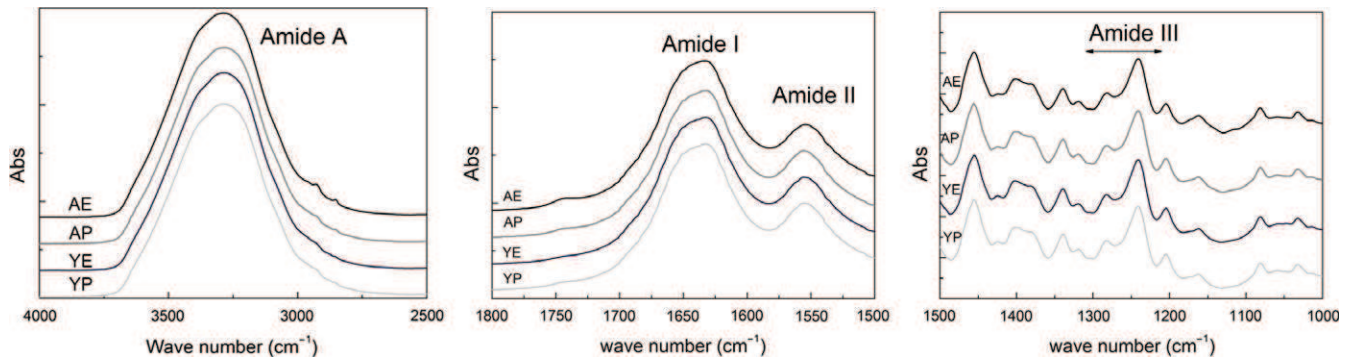
FIGURE 3 Averaged normalized FTIR spectra in the (4000-2800), (1750-1500) and (1500-1000) cm^{-1} regions for a matched set of skin biopsies

non-exposed aged skin (AP, T_{mid}=67.4°C, P=.0313) and the sun-exposed aged skin (AE).

These results could be in favour of a slight fragmentation of the collagen fibres with the cumulative UV exposition during life, which can be attributed to the decrease of unfreezable water observed in sun-exposed skin of aged subjects inducing collagen destabilization as it has been described.[10,25,26]

On the contrary, ΔH is similar in the four series of biopsies with the values of 11.2 (YP), 11.0 (YE), 12.3 (AP) and 11.2 J g^{-1} (AE). A previous

DSC study on collagen rat skin also evidenced that the total denaturation enthalpy did not change with age.[17]

The T_{end} temperature is significantly increased (P=.0184) between the sun-protected skin of young subjects (YP, T_{end}=69.9°C, P=.0184) and the sun-protected skin of elderly subjects (AP, T_{end}=72.3°C). On the contrary, T_{end} is constant for the sun-exposed young and aged skins. Such an increase of the Tend temperature has been already evidenced with age in rat skin,[17] and associated with the increase of heat-stable crosslinks in collagens. In our study, this increase of

TABLE 2 FTIR assignment and approximate descriptions of vibrational modes for human reticular dermis

Band position/cm^{-1}	Assignment
3375-3289	Amide A: mainly ν(N-H) mode of protein with the contribution of the ν(O-H) stretching mode in H$_2$O and polysaccharides
3073	ν(CH) aromatic
3011	ν(=CH) of unsaturated lipids, triglycerides, fatty acids
2957, 2924, 2873, 2852	νas(CH$_3$), νas(CH$_2$), νs(CH$_3$),νs(CH$_2$), (Gly, Pro, Hyp, Ala) of proteins + phospholipids, triglycerides Most representative of proteins: νs(CH$_3$) Most representative of lipids: νas(CH$_2$) and νs(CH$_2$)
1744	ν(C=O) of triglycerides, cholesterol esters, phospholipids
1694-1630	Amide I: ν(C=O) + δ(O-H) water
1558-1542	Amide II: ν(C-N), δ (N-H)
1520, 1515, 1507	Side chains (Tyrosine, Phenylalanine)
1452	δ(CH$_2$) scissoring, δ(CH$_3$) bending of lipids (mainly), proteins
1401-1393	ν_s(COO-) of free amino acids, fatty acid, (GAG)s
1338	δ(CH$_2$) wagging of proline chain Specific band of collagen (and elastin with a minor contribution)
1310-1202	Amide III δ_{plan} (N-H) and ν(C-N) of proteins 1238 cm^{-1}: specific of ECM (collagen) 1205 cm^{-1}: specific of ECM (collagen)
1246-1235	νas(PO$_2^-$) stretching of phospholipids, nucleic acids
1250-1210	νas(SO$_3^-$) sulfated (GAG)s
1167-1156	ν_{as}(CO-O-C) cholesterol esters, phospholipids
1200-1000	ν(C-O), ν(C-C), ν(C-OH), ν(C-O-C) of proteins, oligosaccharides, glycolipids 1171 cm^{-1}: νas(CO-O-C) of cholesterol esters 1159 cm^{-1}: ν(C-OH) of Hyp and nucleic acids 1115 cm^{-1}: ν (C-O) carbohydrates 1081 cm^{-1}: ν(C-O-C) collagen, glycogen, oligosaccharides, glycolipids, proteoglycans, and νs(PO$_2^-$) nucleic acids, phospholipids 1032 cm^{-1}: νs(CO-O-C) of carbohydrates residues of collagen, (GAG)s, νs(SO$_3^-$) (GAG)s

heat-stable crosslinks seems to be achieved mainly by the chronological ageing. From these results, we can hypothesize that age-induced glycation products and/or carbonyl changes could be one of the post-translational modifications of chronological ageing.[27,28]

3.4 | Vibrational characterization

Native biological tissues at a constant hydration can be directly analysed by FTIR in the ATR mode without any other preparation. This technique is widely applied to investigate in vivo or in vitro the outermost layer of human skin, that is, the stratum corneum,[29–32] but few data are available on the internal layer of human skin, that is, the reticular dermis. The measuring depth of ATR-FTIR in the skin is typically a few microns over the wave number window 4000–650 cm^{-1}.[32]
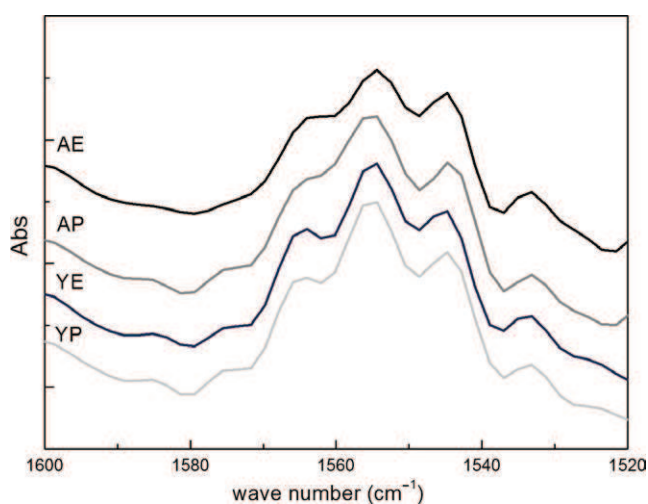

FIGURE 4 Averaged FSD spectra computed from the individual FTIR spectra of skin biopsies in the (1600-1520) cm^{-1} region

Mean FTIR spectra of the skin biopsies are collected in Figure 3. Table 2 summarizes IR bands present in the reticular dermis of the four types of biopsies. Peaks assignments were realized according to literature data on proteins [33] such as collagen [34–36] and biological tissues [37] such as dermis.[38]

The classical absorption bands of proteins (amide A, amide I, II, III) are found on the spectra of the four series of biopsies and their positions are very close to the absorption bands of pure type I collagen. Notably, collagen absorption features in the fingerprint region (the specific triplet of bands at 1204, 1239 and 1282 cm^{-1} [37] as well as the specific band at 1338 cm^{-1} [8,37] are found in dermis samples, and the correlation coefficient between collagen and dermis spectra is more than 0.95 in this region. It must be pointed out that the Amide II is slightly shifted towards low wave numbers (2 cm^{-1}) in the sun exposed skin of elderly subject. This shift is associated with a change in intensity of the different components of the amide II as seen in the FSD spectra (Figure 4).

In a previous work on human skin biopsies we evidenced a pronounced shift of the Amide II band towards low wavenumber in heat-denatured derma [20] and it was attributed to the depletion of the triple helical structure of collagen and the enhancement of disordered structures.[36] In sun-exposed skin biopsies, this slight shift of the amide II must be correlated to the thermal evolution of the collagen denaturation evidencing a destabilization of the triple helix domain of collagen.

In order to quantify the variation of the vibrational answer of the different skin biopsies, the area of the different absorption bands were computed from the individual spectrum of each tissue and the appropriate ratio of areas were performed according to the literature data.[37,39,40] The most relevant indicators are displayed in Figure 5.

As shown in Figure 5A, a significant drastic decrease (−16%, P=.0489) of the area ratio (1338 cm^{-1})/(1750-1000 cm^{-1}), is evidenced in sun-exposed aged skin (AE) compared with sun-exposed
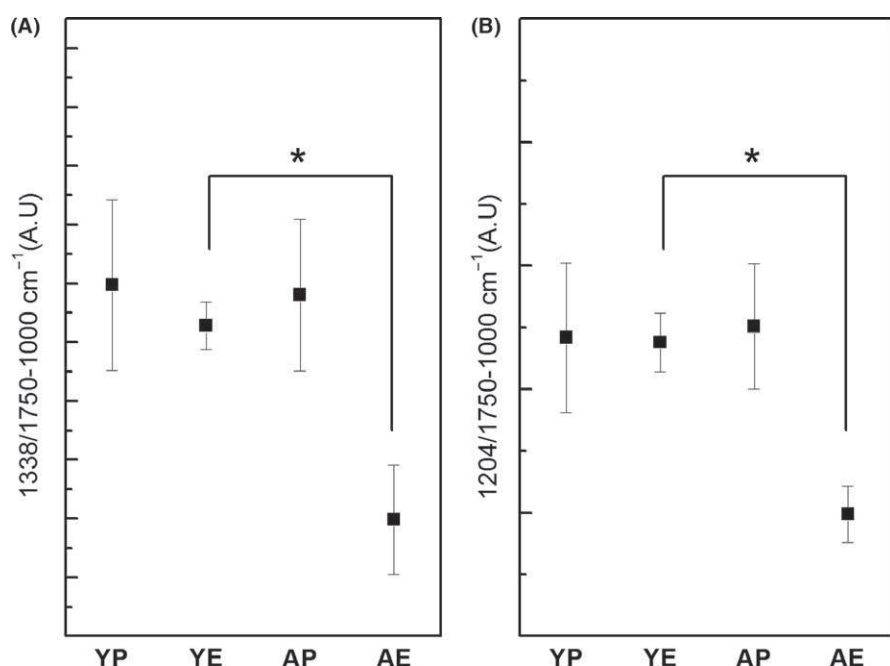

FIGURE 5 Area ratios of the different absorption bands from FTIR spectra: A, Area ratio (1338 cm^{-1})/(1750-1000 cm^{-1}) and B, Area ratio (1204 cm^{-1})/(1750-1000 cm^{-1})

young skin (YE). This indicator is proportional to fibrillary collagen content, the main protein component of dermis. However, with age no significant difference was observed on non-exposed area. This is corroborated by a similar evolution of the area ratio (1204 cm^{-1})/(1750-1000 cm^{-1}), another marker of the ECM proteins amount (Figure 5B) (−18%, P=.0239). These area ratio evolutions are consistent with the literature data, showing alterations in the amount and architecture of collagen content in human dermis under extrinsic ageing.[26]

4 | CONCLUSION

DSC is a powerful technique to evaluate the hydric organization of human dermis and the collagen stability. For the first time, a direct quantification of freezable and unfreezable water in human skin biopsies from two age groups has been achieved. Photoageing induces a decrease of unfreezable water and an increase of freezable water, highlighting the predominant role of extrinsic ageing on water organization in human skin. Moreover, photoageing-induced decrease collagen stability could be explained by the detriment of interaction bounded-water to protein and/or collagen fragmentation. In contrast, chronological ageing-increased collagen stability could be due to age-induced glycation and carbonyl modifications. These alterations of the collagenic fraction with extrinsic ageing are confirmed by the decrease of the specific vibrational signature of fibrillar collagens in dermis as shown by FTIR analysis. These results are promising for the identification of new biomarkers of ageing in a future work exploring the skin at different depth levels with Raman confocal microscopy, a technique which becomes more frequent for biological analysis.

REFERENCES

1. Jung JW, Cha S-H, Lee S-C, Chun I-K, Kim Y-P. Age-related changes of water content in the rat skin. *J Dermatol Sci*. 1997;14:12-19.
2. Carrino DA, Onnerfjord P, Sandy JD, et al. Age-related changes in the proteoglycans of human skin. Specific cleavage of decorin to yield a major catabolic fragment in adult skin. *J Biol Chem*. 2003;278:17566-17572.
3. Ngan CL, Basri M, Tripathy M. Abedi Karjiban R, Abdul-Malek E. Skin intervention of fullerene-integrated nanoemulsion in structural and collagen regeneration against skin aging. *Eur J Pharm Sci*. 2015;70:22-28.
4. Krieg T, Aumailley M. The extracellular matrix of the dermis: flexible structures with dynamic functions. *Exp Dermatol*. 2011;20:689-695.
5. Waller JM, Maibach HI. Age and skin structure and function, a quantitative approach (II): protein, glycosaminoglycan, water, and lipid content and structure. *Skin Res Technol*. 2006;12:145-154.
6. Kammeyer A, Luiten RM. Oxidation events and skin aging. *Ageing Res Rev*. 2015;21C:16-29.
7. Miyamae Y, Yamakawa Y, Kawabata M, Ozaki Y. A combined near-infrared diffuse reflectance spectroscopy and principal component analysis method of assessment for the degree of photoaging and physiological aging of human skin. *Anal Sci*. 2012;28:1159-1164.
8. Canuto HC, Fishbein KW, Huang A, et al. Characterization of skin abnormalities in a mouse model of osteogenesis imperfecta using high resolution magnetic resonance imaging and Fourier transform infrared imaging spectroscopy. *NMR Biomed*. 2012;25:169-176.
9. Nakagawa N, Matsumoto M, Sakai S. In vivo measurement of the water content in the dermis by confocal Raman spectroscopy. *Skin Res Technol*. 2010;16:137-141.
10. Gniadecka M, Nielsen OF, Wessel S, Heidenheim M, Christensen DH, Wulf HC. Water and protein structure in photoaged and chronically aged skin. *J Invest Dermatol*. 1998;111:1129-1133.
11. Wright AC, Bohning DE, Pecheny AP, Spicer KM. Magnetic resonance chemical shift microimaging of aging human skin in vivo: initial findings. *Ski Res Technol*. 1998;4:55-62.
12. Zhang Q, Andrew Chan KL, Zhang G, et al. Raman microspectroscopic and dynamic vapor sorption characterization of hydration in collagen and dermal tissue. *Biopolymers*. 2011;95:607-615.
13. Aktas N, Tülek Y, Gökalp HY. Determination of freezable water content of beef semimembranous muscle DSC study. *J Therm Anal*. 1997;48:259-266.
14. Miles CA, Burjanadze TV, Bailey AJ. The kinetics of the thermal denaturation of collagen in unrestrained rat tail tendon determined by differential scanning calorimetry. *J Mol Biol*. 1995;245:437-446.
15. Samouillan V, Delaunay F, Dandurand J, et al. The Use of Thermal Techniques for the Characterization and Selection of Natural Biomaterials. *J Funct Biomater*. 2011;2:230-248.
16. Miles CA, Avery NC. Thermal stabilization of collagen in skin and decalcified bone. *Phys Biol*. 2011;8:26002.
17. Flandin F, Buffevant C, Herbage D. A differential scanning calorimetry analysis of the age-related changes in the thermal stability of rat skin collagen. *Biochim Biophys Acta - Protein Struct Mol Enzymol*. 1984;791:205-211.
18. Le Lous M, Flandin F, Herbage D, Allain JC. Influence of collagen denaturation on the chemorheological properties of skin, assessed by differential scanning calorimetry and hydrothermal isometric tension measurement. *Biochim Biophys Acta - Gen Subj*. 1982;717:295-300.
19. Wiegand N, Naumov I, Nőt LG, Vámhidy L, Lőrinczy D. Differential scanning calorimetric examination of pathologic scar tissues of human skin. *J Therm Anal Calorim*. 2012;111:1897-1902.
20. Tang R, Samouillan V, Dandurand J, et al. Thermal and vibrational characterization of human skin. *J Therm Anal Calorim*. 2016;16:1-12.
21. Heys KR, Friedrich MG, Truscott RJW. Free and bound water in normal and cataractous human lenses. *Invest Ophthalmol Vis Sci*. 2008;49:1991-1997.
22. Verdier-Sévrain S, Bonté F. Skin hydration: a review on its molecular mechanisms. *J Cosmet Dermatol*. 2007;6:75-82.
23. Bohning DE, Pecheny AP, Wright AC, Spicer KM. Magnetic resonance coil for 31 P spectroscopy of skin over curved body surfaces. *Skin Res Technol*. 1998;4:63-70.
24. Gniadecka M, Jemec GB. Quantitative evaluation of chronological ageing and photoageing in vivo: studies on skin echogenicity and thickness. *Br J Dermatol*. 1998;139:815-821.
25. Bella J, Brodsky B, Berman HM. Hydration structure of a collagen peptide. *Structure*. 1995;3:893-906.
26. Bernstein EF, Chen YQ, Kopp JB, et al. Long-term sun exposure alters the collagen of the papillary dermis. Comparison of sun-protected and photoaged skin by northern analysis, immunohistochemical staining, and confocal laser scanning microscopy. *J Am Acad Dermatol*. 1996;34:209-218.
27. Tanase M, Urbanska AM, Zolla V, et al. Role of Carbonyl Modifications on Aging-Associated Protein Aggregation. *Sci Rep*. 2016;6:19311.
28. Gkogkolou P, Böhm M. Advanced glycation end products: key players in skin aging? *Dermatoendocrinol*. 2012;1:259-270.
29. Pouliot R, Germain L, Auger FA, Tremblay N, Juhasz J. Physical characterization of the stratum corneum of an in vitro human skin equivalent produced by tissue engineering and its comparison with normal human skin by ATR-FTIR spectroscopy and thermal analysis (DSC). *Biochim Biophys Acta*. 1999;18:341-352.

30. Takada S, Naito S, Sonoda J, Miyauchi Y. Noninvasive In Vivo Measurement of Natural Moisturizing Factor Content in Stratum Corneum of Human Skin by Attenuated Total Reflection Infrared Spectroscopy. *Appl Spectrosc*. 2012;66:26-32.

31. Brancaleon L, Bamberg MP, Sakamaki T, Kollias N. Attenuated Total Reflection Fourier Transform Infrared Spectroscopy as a Possible Method to Investigate Biophysical Parameters of Stratum Corneum In Vivo. *J Invest Dermatol*. 2001;380-386.

32. Lucassen GW, van Veen GN, Jansen JA. Band analysis of hydrated human skin stratum corneum attenuated total reflectance fourier transform infrared spectra in vivo. *J Biomed Opt*. 1998;3:267-280.

33. Barth A. Infrared spectroscopy of proteins. *Biochim Biophys Acta*. 2007;1767:1073-1101.

34. Structures Protein FTIR Data Analysis and Band Assignment. *Acta bioch Biophys Sin*. 2007;39:549-559.

35. Belbachir K, Noreen R, Gouspillou G, Petibois C. Collagen types analysis and differentiation by FTIR spectroscopy. *Anal Bioanal Chem*. 2009;395:829-837.

36. Payne KJ, Veis A. Fourier transform IR spectroscopy of collagen and gelatin solutions: deconvolution of the amide I band for conformational studies. *Biopolymers*. 1988;27:1749-1760.

37. Rabotyagova OS, Cebe P, Kaplan DL. Collagen Structural Hierarchy and Susceptibility to Degradation by Ultraviolet Radiation. *Mater Sci Eng C Mater Biol Appl*. 2008;28:1420-1429.

38. Staniszewska E, Malek K, Baranska M. Rapid approach to analyze biochemical variation in rat organs by ATR FTIR spectroscopy. *Spectrochim Acta - Part A Mol Biomol Spectrosc*. 2014;24:981-986.

39. Tfayli A, Piot O, Durlach A, Bernard P, Manfait M. Discriminating nevus and melanoma on paraffin-embedded skin biopsies using FTIR microspectroscopy. *Biochim Biophys Acta*. 2005;1724:262-269.

40. Wang Q, Sanad W, Miller LM, et al. Infrared imaging of compositional changes in inflammatory cardiomyopathy. *Vib Spectrosc*. 2005;38:217-222.